

Cite this: *Chem. Sci.*, 2023, 14, 705

All publication charges for this article have been paid for by the Royal Society of Chemistry

Received 29th September 2022  
Accepted 6th December 2022

DOI: 10.1039/d2sc05428k

rsc.li/chemical-science

# Cu-catalyzed enantioselective decarboxylative cyanation *via* the synergistic merger of photocatalysis and electrochemistry†

Yin Yuan,<sup>a</sup> Junfeng Yang<sup>ID</sup>\*<sup>ab</sup> and Junliang Zhang<sup>ID</sup>\*<sup>a</sup>

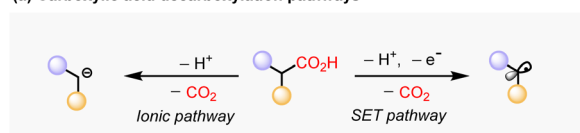
The development of an efficient and straightforward method for decarboxylative coupling using common alkyl carboxylic acid is of great value. However, decarboxylative coupling with nucleophiles always needs stoichiometric chemical oxidants or substrate prefunctionalization. Herein, we report a protocol for Cu-catalyzed enantioselective decarboxylative cyanation *via* the merger of photocatalysis and electrochemistry. CeCl<sub>3</sub> and Cu/BOX were used as co-catalysts to promote the decarboxylation and cyanation, and both catalysts were regenerated *via* anodic oxidation. This method establishes a proof of concept enantioselective transformation *via* photoelectrocatalysis. Studies by DFT calculations provided mechanistic insight on enantioselectivity control.

## Introduction

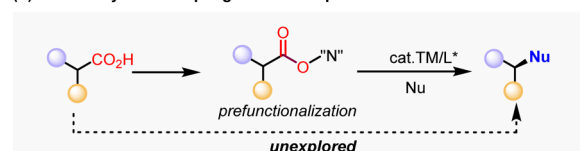
Carboxylic acids are widely available and fundamental chemical feedstocks which are produced in huge amounts.<sup>1</sup> Many alkyl carboxylic acids exist in nature as biomass and in a renewable form (*e.g.* amino acid, fatty acid, peptides and sugar acids).<sup>2</sup> In this regard, the abundance of alkyl carboxylic acids makes it an attractive precursor in carbon–carbon or carbon–heteroatom bond-formation processes through decarboxylation.<sup>3–5</sup> Much effort has been devoted to decarboxylative coupling methods, either by an ionic pathway<sup>3,5</sup> or single electron transfer (SET) pathway conceptually (Scheme 1a).<sup>4</sup> The ionic pathway is promoted thermally by transition metals<sup>3</sup> or organocatalysis,<sup>5</sup> with most substrates being limited to electron-deficient substrates that facilitate anionic decarboxylation. Instead of generating an anion intermediate, the SET pathway involves the single-electron oxidation process to give alkyl radicals, either through a Hunsdiecker type process<sup>6</sup> or photoredox-catalytic approach,<sup>4a,7</sup> which were subsequently intercepted by radical acceptors. This approach is particularly useful in enantioselective carbon–carbon bond-forming reactions with electrophilic organohalides *via* a redox-neutral strategy.<sup>7e,7f</sup> However, enantioselective decarboxylative carbon–heteroatom bond-formation reactions always require an oxidizing agent,<sup>8</sup> or the prefunctionalization of the carboxylic acids<sup>9</sup> to facilitate the decarboxylative generation of alkyl radical *via* single electron reduction of carboxylic acid derivatives, such as redox-active

esters.<sup>4a,7a</sup> Seminal work by G. Liu and coworkers has demonstrated the enantioselective cyanation of redox-active esters by Ir photoredox catalysis and Cu catalysis.<sup>10</sup> However, this protocol increases the synthetic effort and deteriorates the atom economy. In this context, enantioselective decarboxylative

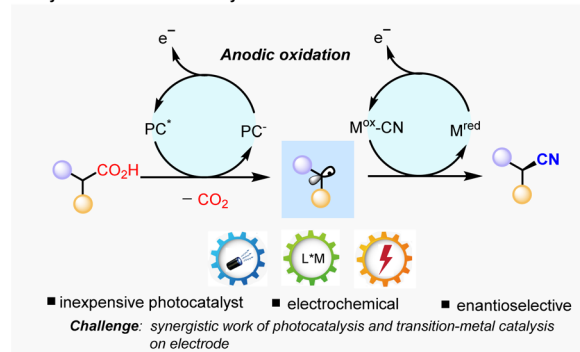
### (a) Carboxylic acid decarboxylation pathways



### (b) Decarboxylative coupling with nucleophiles:



### (c) Design: synergistic merger of photocatalyst, transition metal catalyst and electrochemistry



Scheme 1 Background and project synopsis.

<sup>a</sup>Department of Chemistry, Fudan University, 2005 Songhu Road, Shanghai, 200438, P. R. China. E-mail: junliangzhang@fudan.edu.cn

<sup>b</sup>Fudan Zhangjiang Institute, Shanghai 201203, P. R. China

† Electronic supplementary information (ESI) available. See DOI: <https://doi.org/10.1039/d2sc05428k>

coupling with nucleophiles directly through simple alkyl carboxylic acids remains elusive (Scheme 1b).

Recently, electrochemistry has gained increasing attention as a sustainable approach for organic synthesis owing to its ability to generate highly reactive radical intermediates by SET on electrodes.<sup>11</sup> In addition, the ability to control redox potential at the minimum level required for the desired redox transformation makes it an attractive approach of functionalizing complex synthetic intermediates. Therefore, we seek to use electrochemistry as a practical strategy to furnish the decarboxylation and regeneration of catalysis on electrodes. However, direct electrolysis of carboxylic acids (Kolbe electrolysis) suffers from poor selectivity, as the alkyl radical species tend to undergo dimerization or further oxidation to give alkyl cations, which would give a mixture of alkenes and racemic products.<sup>12</sup> Inspired by the unique performance of  $\text{CeCl}_3$  as an efficient photocatalyst to promote decarboxylation<sup>13</sup> and the good performance of Cu as a catalyst in radical coupling,<sup>14</sup> as well as the similar redox potentials of  $\text{CeCl}_3$  and  $\text{Cu(II)}$  by anodic oxidation,<sup>15</sup> we envision a synergistic approach to conduct enantioselective decarboxylative cyanation *via* the merger of photocatalysis and electrochemistry.<sup>16</sup> If successful, the developed methodology would be highly valuable, because it avoids the usage of stoichiometric oxidants, prefunctionalized substrates and noble photocatalysts. The main challenge in this

scenario lies in the synergistic work of photochemistry, electrochemistry, and parallel generation of two catalytic species, in other words, the compatibility of photoredox-induced radical generation and electrochemically catalyst regeneration. Herein, we disclose copper catalyzed enantioselective decarboxylative cyanation *via* electrochemistry and photocatalysis (Scheme 1c).

## Results and discussion

We commenced the enantioselective electrophotocatalytic decarboxylative cyanation using phenylpropanoic acids (**1a**) and TMSCN as starting materials (Table 1). A 465 nm blue LED was employed as the light source. Commercially inexpensive  $\text{CeCl}_3 \cdot 7\text{H}_2\text{O}$  was found to be an efficient photocatalyst compared with other Ce sources (Table 1, entry 2). After extensive screening, the optimal reaction condition was established using 5 mol% of  $\text{Cu(hfacac)}_2 \cdot \text{H}_2\text{O}$  as a catalyst, 6 mol% of chiral bidentate BOX ligand (**L5**), 10 mol% of  $\text{CeCl}_3 \cdot 7\text{H}_2\text{O}$  as a cocatalyst, 2.0 equiv. of  $n\text{-Bu}_4\text{NPF}_6$  as supporting electrolyte, pyridine as the base and  $\text{CH}_3\text{CN}$  as solvent in an undivided cell exposed to a 465 nm LED (40 W). Under the optimal conditions, the desired cyanation product **2a** was isolated in 77% yield with 92% ee. A series of BOX ligands were examined, including those commonly used with the combination of Cu as Lewis acid or radical catalysis. **L5** proved to be the best one, delivering the

Table 1 Optimization of reaction conditions<sup>a</sup>

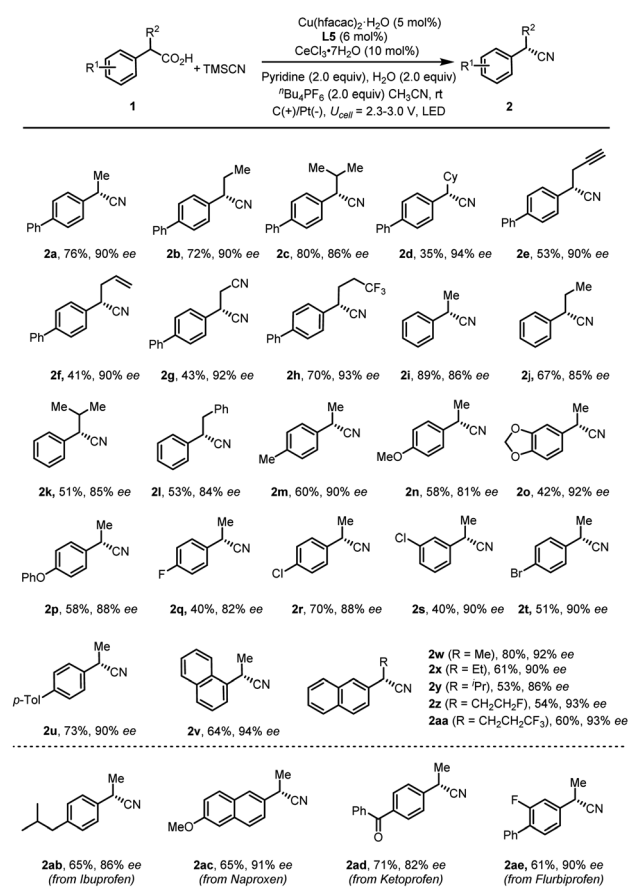
Entry	Deviation from the standard conditions	Yield <sup>b</sup> [%]	ee <sup>c</sup> [%]
1	None	77	92
2	$\text{Ce}_2\text{SO}_4$ (10 mol%) instead of $\text{CeCl}_3 \cdot 7\text{H}_2\text{O}$	Trace	—
3	$\text{Cs}_2\text{CO}_3$ instead of pyridine	NR	—
4	Pyridine (50 mol%) was used	36	92
5	No pyridine	NR	—
6	DMF as solvent	Trace	—
7	No $\text{H}_2\text{O}$	73	90
8	Ni foam (0.5 cm × 2 cm) was used as cathode	NR	—
9	$U_{\text{cell}} = 3.0$ V	58	89
10	$\text{Cu(OTf)}_2$ instead of $\text{Cu(hfacac)}_2 \cdot \text{H}_2\text{O}$	45	90
11	Under air	43	91
12	No LEDs	NR	—
13	No electricity	NR	—
14	No $\text{CeCl}_3 \cdot 7\text{H}_2\text{O}$	Trace	—
15	No Cu	NR	—
16	$\text{CeCl}_3 \cdot 7\text{H}_2\text{O}$ (5 mol%) was used	44	91



<sup>a</sup> The reaction was performed using 0.2 mmol of **1a** (0.05 M), 0.4 mmol TMSCN (0.1 M),  $\text{Cu(hfacac)}_2 \cdot \text{H}_2\text{O}$  (5 mol%), **L5** (6 mol%),  $\text{H}_2\text{O}$  (2 equiv.)  $n\text{-Bu}_4\text{NPF}_6$  (0.4 mmol) and  $\text{CH}_3\text{CN}$  (4 mL) in an undivided cell with a carbon felt anode and Pt cathode under constant cell potential conditions with irradiation for 6 h. <sup>b</sup> Yield was determined by GC using anisole as an internal standard. NR = no reaction. <sup>c</sup> Determined by HPLC using a chiral stationary phase.



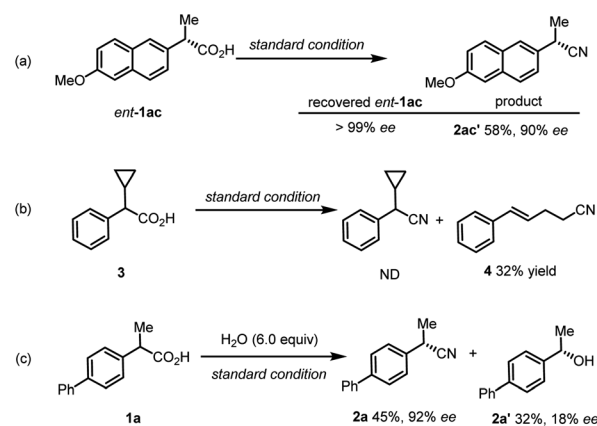
product with 92% ee. A DFT study disclosed that the non-covalent interaction between the indane structure of the ligand and the arene of the substrates is responsible for the high enantioselectivity (*vide infra*). The reaction is an overall oxidative transformation, which requires the proton as the electron scavenger. A batch of additives are examined as the electron scavenger and 2.0 equiv. of H<sub>2</sub>O proved to be beneficial for the yield and ee (Table 1, entry 7, see Table S4† for details). As for the electrode, replacing the Pt cathode with Ni (Table 1, entry 8) or other cathodes shows negative effects on the reaction efficiency. Moreover, further optimization revealed that the copper catalyst has a significant effect on the reactivity and Cu(hfacac)<sub>2</sub>·H<sub>2</sub>O gave the highest yield (Table 1, entry 10, see Table S5† for details). Conducting the reaction under air deteriorated the product formation (Table 1, entry 11). Control experiments indicated that light irradiation (Table 1, entry 12), electricity (Table 1, entry 13), the cerium catalyst (Table 1, entry 14) and Cu catalyst (Table 1, entry 15) were all critical for the reaction to proceed, as omission of any of these results in no desired decarboxylative cyanation product. Furthermore, lowering the Ce loading to 5 mol% results in decreased yield (Table 1, entry 15). This result highlights the importance of balancing the rates of the decarboxylation and cyanation process to ensure the optimal product selectivity.



Scheme 2 Scope of carboxylic acids. The reaction was performed on a 0.2 mmol scale under the conditions in Table 1, entry 1.

With the optimized conditions in hand, we examined the scope of carboxylic acids in this reaction (Scheme 2). We were gratified to find that benzyl carboxylic acids featuring linear and branched aliphatic side chains were all suitable substrates for this reaction (2a–2d). Additionally, substituents such as terminal alkyne (2e), alkene (2f), cyanide (2g), and trifluoromethyl groups (2h) on the alkyl side chains were all tolerated. On the other hand, various functional groups of either electron-rich or -poor group on the phenyl rings of benzyl carboxylic acids were compatible under the current reaction conditions. In particular, functional groups that are susceptible to undergo oxidative degradation, such as electro-rich arenes (2m–2p) can be tolerated, delivering cyanation products in moderate to good yield with good enantioselectivity. Notably, halide groups, such as the chloride and bromide are well tolerated (2r–2t), which allows for further transformation by a cross-coupling reaction. Gratifyingly, commercially available racemic arylpropanoic acids, also known as nonsteroidal anti-inflammatory drugs, such as ibuprofen (1ab), naproxen (1ac), Ketoprofen (1ad) and flurbiprofen (1ae), were suitable substrates to deliver enantiomer enriched benzylic nitriles in good yields with good enantioselectivities (2ab–2ae). However, non-benzyl carboxylic acids are not competent substrates under the optimized conditions, probably due to the low stability of the radical intermediate.

To obtain experimental support for the mechanistic insight into this reaction, we conducted a few control experiments (Scheme 3). Firstly, when (*S*)-naproxen (ent-1ac) was used as the starting material, the same enantioselective product 2ac could be obtained (Scheme 3a). Meanwhile, no racemization of the starting material occurs under the reaction condition. This result revealed that the chiral ligand effectively controls the absolute configuration of the product, regardless of the stereochemistry of the electrophile, and that decarboxylation is essentially irreversible. Secondly, the reaction of radical clock substrate 3 under the standard conditions delivered a major ring-opening/cyanation product 4 in 32% yield with no detection of desired decarboxylative cyanation product (Scheme 3b). This result can serve as the direct evidence of the radical intermediate. Thirdly, when excessive water (6.0 equiv.) was



Scheme 3 Mechanistic studies.

added into the model reaction as the additive, we observed a high ratio of hydroxylation product with 18% ee (Scheme 3c), which is intriguing and provides the preliminary result for the promising enantioselective hydroxylation.

Based on the above studies and related literature reports,<sup>10,15,17</sup> a possible mechanism for the electro-photocatalytic decarboxylative cyanation was tentatively proposed (Scheme 4a). The reaction commences with the oxidation of Ce(III) to Ce(IV) ( $E_{p/2}^{\text{red}} = 0.38 \text{ V vs. Ag/Ag}^+$  in  $\text{CH}_3\text{CN}$ ) on the anode.<sup>13</sup> The resulting Ce(IV) species coordinates with the carboxylic acid to give complex **A**, which then undergoes the photoinduced ligand-to-metal charge transfer (LMCT) to deliver the carboxylic radical **B** and the reduced Ce(III) species.<sup>18</sup> The subsequent decarboxylation would generate the benzylic radical, which undergoes single-electron oxidative addition to the  $\text{L}^*\text{Cu(I)CN}$  species, affording the alkyl- $\text{L}^*\text{Cu(III)}$  CN species. This event is followed by inner sphere reductive elimination to furnish the chiral cyanation product and regenerate the Cu(I) catalyst. Cu(I) species further undergoes anodic oxidation and combines with another  $\text{CN}^-$  to give  $\text{L}^*\text{Cu(II)CN}$  species. The possibility of the oxidation of Ce(III) by  $\text{L}^*\text{Cu(III)CN}$  may be speculated. We measured the redox potentials of the different reaction species as shown in Scheme 4b using cyclic voltammetry (CV) data and found that the oxidation of the  $\text{L}^*\text{Cu(I)CN}$  catalyst to the corresponding  $\text{L}^*\text{Cu(II)CN}$  occurred at around 0.42 V (vs.  $\text{Ag/Ag}^+$ ). A visible drop of current is observed with the addition of  $\text{CeCl}_3$  (Scheme 4b), which may be attributed to the interaction between Ce(IV) and Cu(I). As a result, the

oxidation of Cu(I) species by Ce(IV) cannot be excluded. It should also be noted that the complexation of Ce(III) with the carboxylic acid before the anode oxidation is highly possible based on the comparison of the CV data of  $\text{CeCl}_3$  and  $\text{CeCl}_3$  with **1a**.

Even though the BOX ligand **L5** has been extensively used in the Cu-catalyzed radical coupling reaction, the explanation of the stereo control of the ligand has not been well studied. A previous report has shown that the radical combination of a benzylic radical with  $\text{L}^*\text{Cu(III)CN}$  is facile.<sup>17b</sup> Thus, we performed DFT calculations on the C–C reductive elimination to elucidate the role of the ligand in enantioselectivity. The calculations showed that the two transition states differ in free energy of activation by 2.2 kcal mol<sup>−1</sup> favoring the S product, which is in good agreement with the experiments (Scheme 4c). In addition, the IGM analysis showed that C–H⋯π interactions between the benzylic proton of the ligand and the aryl group of the substrate plays a significant role in lowering the energy of the transition state (Scheme 4c, see the ESI† for details).<sup>15b</sup> This interaction could be further proved by our experimental observation that higher enantioselectivity could be obtained with a substrate containing more electro-rich aryl group. For example, substrates with a *para*-phenyl group (**1a**) or naphthyl group (**1v–1aa**) afforded higher ee than the parent phenyl substrate (**1i**).

## Conclusions

In summary, we have developed a Cu-catalyzed enantioselective decarboxylative cyanation reaction in a synergistic fashion with the merger of photocatalysis and electrochemistry, which allows the direct decarboxylation coupling of simple carboxylic acids.<sup>19</sup> The current work demonstrates that this synergistic fashion could avoid the need for stoichiometric chemical oxidants or substrate prefunctionalization, in the meantime, enabling the reaction to operate under mild condition with high enantioselectivity and a reasonable range of functionalities. Further synthetic and mechanistic explorations of photoelectrocatalysis are currently underway.

## Data availability

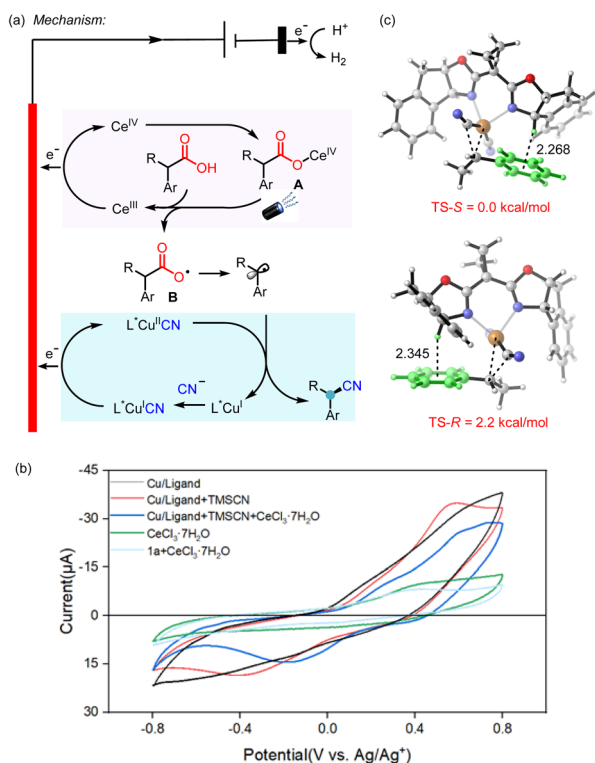
All of the experimental and computational data is available and has been included in the ESI† of this publication.

## Author contributions

Y. Yuan conducted most of the reactions, experimental mechanistic studies and full characterization of the compounds. J. Yang conceptualized and directed the project, performed the DFT calculations and wrote the manuscript. All authors contributed to scientific discussions.

## Conflicts of interest

There are no conflicts to declare.



Scheme 4 Proposed catalytic cycle, DFT study and cyclic voltammetry data.





## Acknowledgements

We gratefully acknowledge the funding support of the National Key R&D Program of China (2021YFF0701600), NSFC (21901043, 21921003, and 22031004), STCSM (21ZR1445900) and Shanghai Municipal Education Commission (20212308).

## Notes and references

- 1 A. J. J. Straathof, *Chem. Rev.*, 2014, **114**, 1871–1908.
- 2 E. Scott, F. Peter and J. Sanders, *Appl. Microbiol. Biotechnol.*, 2007, **75**, 751–762.
- 3 For recent reviews, see: (a) N. Rodríguez and L. J. Goossen, *Chem. Soc. Rev.*, 2011, **40**, 5030–5048; (b) J. D. Weaver, A. Recio iii, A. J. Grenning and J. A. Tunge, *Chem. Rev.*, 2011, **111**, 1846–1913; (c) Y. Wei, P. Hu, M. Zhang and W. Su, *Chem. Rev.*, 2017, **117**, 8864–8907; (d) P. J. Moon and R. J. Lundgren, *ACS Catal.*, 2020, **10**, 1742–1753.
- 4 For recent reviews, see: (a) J. Xuan, Z.-G. Zhang and W.-J. Xiao, *Angew. Chem., Int. Ed.*, 2015, **54**, 15632–15641; (b) Y. Jin and H. Fu, *Asian J. Org. Chem.*, 2017, **6**, 368–385; (c) Y. Li, L. Ge, M. T. Muhammad and H. Bao, *Synthesis*, 2017, **49**, 5263–5284; (d) T. Patra and D. Maiti, *Chem.-Eur. J.*, 2017, **23**, 7382–7401; (e) J. Schwarz and B. König, *Green Chem.*, 2018, **20**, 323–361.
- 5 S. Nakamura, *Org. Biomol. Chem.*, 2014, **12**, 394–405.
- 6 (a) X. Liu, Z. Wang, X. Cheng and C. Li, *J. Am. Chem. Soc.*, 2012, **134**, 14330–14333; (b) Z. Wang, L. Zhu, F. Yin, Z. Su, Z. Li and C. Li, *J. Am. Chem. Soc.*, 2012, **134**, 4258–4263; (c) F. Yin, Z. Wang, Z. Li and C. Li, *J. Am. Chem. Soc.*, 2012, **134**, 10401–10404; (d) C. Liu, X. Wang, Z. Li, L. Cui and C. Li, *J. Am. Chem. Soc.*, 2015, **137**, 9820–9823; (e) X. Tan, Z. Liu, H. Shen, P. Zhang, Z. Zhang and C. Li, *J. Am. Chem. Soc.*, 2017, **139**, 12430–12433.
- 7 For reviews and leading references, see: (a) S. Murarka, *Adv. Synth. Catal.*, 2018, **360**, 1735–1753; (b) A. Noble, R. S. Mega, D. Pflästerer, E. L. Myers and V. K. Aggarwal, *Angew. Chem., Int. Ed.*, 2018, **57**, 2155–2159; (c) C. Shu, R. S. Mega, B. J. Andreassen, A. Noble and V. K. Aggarwal, *Angew. Chem., Int. Ed.*, 2018, **57**, 15430–15434; (d) R. S. Mega, V. K. Duong, A. Noble and V. K. Aggarwal, *Angew. Chem., Int. Ed.*, 2020, **59**, 4375–4379; (e) Z. Zuo, H. Cong, W. Li, J. Choi, G. C. Fu and D. W. C. MacMillan, *J. Am. Chem. Soc.*, 2016, **138**, 1832–1835; (f) C. Pezzetta, D. Bonifazi and R. W. M. Davidson, *Org. Lett.*, 2019, **21**, 8957–8961.
- 8 G. a. Zhang, P. Huang, Z. Li, J. Guo, Y. Pei, M. Li, W. Ding and J. Wu, *Cell Rep. Phys. Sci.*, 2022, **3**, 101104.
- 9 Z. Zeng, A. Feceu, N. Sivendran and L. J. Gooßen, *Adv. Synth. Catal.*, 2021, **363**, 2678–2722.
- 10 D. Wang, N. Zhu, P. Chen, Z. Lin and G. Liu, *J. Am. Chem. Soc.*, 2017, **139**, 15632–15635.
- 11 For recent reviews see: (a) A. Jutand, *Chem. Rev.*, 2008, **108**, 2300–2347; (b) J.-i. Yoshida, K. Kataoka, R. Horcajada and A. Nagaki, *Chem. Rev.*, 2008, **108**, 2265–2299; (c) R. Francke and R. D. Little, *Chem. Soc. Rev.*, 2014, **43**, 2492–2521; (d) M. Yan, Y. Kawamata and P. S. Baran, *Chem. Rev.*, 2017, **117**, 13230–13319; (e) M. D. Karkas, *Chem. Soc. Rev.*, 2018, **47**, 5786–5865; (f) K. Liu, C. Song and A. Lei, *Org. Biomol. Chem.*, 2018, **16**, 2375–2387; (g) S. Möhle, M. Zirbes, E. Rodrigo, T. Gieshoff, A. Wiebe and S. R. Waldvogel, *Angew. Chem., Int. Ed.*, 2018, **57**, 6018–6041; (h) C. Sandford, M. A. Edwards, K. J. Klunder, D. P. Hickey, M. Li, K. Barman, M. S. Sigman, H. S. White and S. D. Minter, *Chem. Sci.*, 2019, **10**, 6404–6422; (i) H. Wang, X. Gao, Z. Lv, T. Abdelilah and A. Lei, *Chem. Rev.*, 2019, **119**, 6769–6787; (j) C. Kingston, M. D. Palkowitz, Y. Takahira, J. C. Vantourout, B. K. Peters, Y. Kawamata and P. S. Baran, *Acc. Chem. Res.*, 2020, **53**, 72–83; (k) D. Pollok and S. R. Waldvogel, *Chem. Sci.*, 2020, **11**, 12386–12400; (l) C. Ma, P. Fang, Z.-R. Liu, S.-S. Xu, K. Xu, X. Cheng, A. Lei, H.-C. Xu, C. Zeng and T.-S. Mei, *Sci. Bull.*, 2021, **66**, 2412–2429; (m) S.-H. Shi, Y. Liang and N. Jiao, *Chem. Rev.*, 2021, **121**, 485–505; (n) C. Zhu, N. W. J. Ang, T. H. Meyer, Y. Qiu and L. Ackermann, *ACS Cent. Sci.*, 2021, **7**, 415–431.
- 12 (a) H. Kolbe, *Ann. Chem. Pharm.*, 1848, **64**, 339–341; (b) H. Kolbe, *Justus Liebigs Annalen der Chemie*, 1849, **69**, 257–294.
- 13 (a) V. R. Yatham, P. Bellotti and B. König, *Chem. Commun.*, 2019, **55**, 3489–3492; (b) L. McMurray, T. M. McGuire and R. L. Howells, *Synthesis*, 2020, **52**, 1719–1737.
- 14 (a) N. Fu, G. S. Sauer, A. Saha, A. Loo and S. Lin, *Science*, 2017, **357**, 575–579; (b) F. Wang, P. Chen and G. Liu, *Acc. Chem. Res.*, 2018, **51**, 2036–2046; (c) X. Y. Dong, Y. F. Zhang, C. L. Ma, Q. S. Gu, F. L. Wang, Z. L. Li, S. P. Jiang and X. Y. Liu, *Nat. Chem.*, 2019, **11**, 1158–1166.
- 15 (a) N. Fu, L. Song, J. Liu, Y. Shen, J. C. Siu and S. Lin, *J. Am. Chem. Soc.*, 2019, **141**, 14480–14485; (b) L. Song, N. Fu, B. G. Ernst, W. H. Lee, M. O. Frederick, R. A. DiStasio Jr and S. Lin, *Nat. Chem.*, 2020, **12**, 747–754.
- 16 (a) H. Huang, Z. M. Strater, M. Rauch, J. Shee, T. J. Sisto, C. Nuckolls and T. H. Lambert, *Angew. Chem., Int. Ed.*, 2019, **58**, 13318–13322; (b) F. Wang and S. S. Stahl, *Angew. Chem., Int. Ed.*, 2019, **58**, 6385–6390; (c) J. P. Barham and B. König, *Angew. Chem., Int. Ed.*, 2020, **59**, 11732–11747; (d) H. Huang, Z. M. Strater and T. H. Lambert, *J. Am. Chem. Soc.*, 2020, **142**, 1698–1703; (e) H. Kim, H. Kim, T. H. Lambert and S. Lin, *J. Am. Chem. Soc.*, 2020, **142**, 2087–2092; (f) X. L. Lai, X. M. Shu, J. Song and H. C. Xu, *Angew. Chem., Int. Ed.*, 2020, **59**, 10626–10632; (g) L. Niu, C. Jiang, Y. Liang, D. Liu, F. Bu, R. Shi, H. Chen, A. D. Chowdhury and A. Lei, *J. Am. Chem. Soc.*, 2020, **142**, 17693–17702; (h) P. Xu, P. Y. Chen and H. C. Xu, *Angew. Chem., Int. Ed.*, 2020, **59**, 14275–14280; (i) W. Zhang, K. L. Carpenter and S. Lin, *Angew. Chem., Int. Ed.*, 2020, **59**, 409–417.
- 17 (a) D. Wang, F. Wang, P. Chen, Z. Lin and G. Liu, *Angew. Chem., Int. Ed.*, 2017, **56**, 2054–2058; (b) W. Zhang, F. Wang, S. D. McCann, D. Wang, P. Chen, S. S. Stahl and G. Liu, *Science*, 2016, **353**, 1014–1018; (c) J. Li, Z. Zhang, L. Wu, W. Zhang, P. Chen, Z. Lin and G. Liu, *Nature*, 2019, **574**,



- 516–521; (d) G. Zhang, S. Zhou, L. Fu, P. Chen, Y. Li, J. Zou and G. Liu, *Angew. Chem., Int. Ed.*, 2020, **59**, 20439–20444.
- 18 (a) A. Hu, J. J. Guo, H. Pan and Z. Zuo, *Science*, 2018, **361**, 668–672; (b) R. Zhao and L. Shi, *Org. Chem. Front.*, 2018, **5**, 3018–3021; (c) S. Shirase, S. Tamaki, K. Shinohara, K. Hirose, H. Tsurugi, T. Satoh and K. Mashima, *J. Am. Chem. Soc.*, 2020, **142**, 5668–5675.
- 19 During peer review of the manuscript, a similar work was reported by Song and Xu, X.-L. Lai, M. Chen, Y. Wang, J. Song and H.-C. Xu, *J. Am. Chem. Soc.*, 2022, **144**, 20201–20206.

